Supporting Information

Jimura et al. 10.1073/pnas.1002007107

SI Methods

Participants. Participants (mean age = 24.5; range 19–34 years, 14 male, 17 female) in the experiment were right-handed, native English speakers, and free from any history of psychiatric or neurological disorders. Each participant provided written informed consent after additional screening for physical or medical condition affecting eligibility for fMRI. The study protocol was approved in accordance with guidelines instituted by the Washington University Human Research Protection Office. Participants were compensated for their participation ($25/h), plus received an additional monetary bonus for task performance (average ≈$10). One participant was eliminated in the individual difference analyses due to outlier scores on the reward sensitivity scales (see also below).

Materials. Eleven hundred emotionally neutral unique words were selected from the English Lexicon Project at Washington University (ref. 1; http://elexicon.wustl.edu/). These words included nouns, adjectives, and verbs, but no adverbs or plurals. Each word consisted of 1 or 2 syllables [1.44 ± 0.81 (mean ± SD)], and 4–6 letters (5.0 ± 0.81) in length. The frequency of the words was 9.62 ± 1.04 (log-transformed; mean ± SD) based on the Hyperspace Analog to Language (HAL) corpus (2). No words were presented more than once during the experiment.

Visual stimuli were presented by using PsyScope software (3) running on an Apple PowerMac G4. Stimuli were projected to participants with an LCD projector onto a screen positioned at the head end of the magnet. Participants viewed the screen through a mirror attached to the head coil. Behavioral responses were recorded via a hand-held fiber-optic, light-sensitive response system interfaced with the PsyScope Button Box.

Procedure. Fig. S1*B* illustrates a working memory trial, consisting of the following series of events. At the beginning of each trial, a fixation cross was presented for 500 ms, followed by the reward cue presented on the center of the screen for 1,000 ms, indicating the amount of potential monetary reward if participants made a correct response within cut-off time. There were three different possible reward cues: three dollar signs ($$$) indicating a 75-cent (high) potential reward, a single dollar sign ($) indicating a 25-cent (low) potential reward, or a blue square indicating no potential reward. Immediately after the reward cue, the 5-word memory set was presented on the screen for a 2.5-s encoding period. A 3.5-s delay followed which served as a retention interval. After the delay, a probe word was presented for 0.5 s. After probe presentation, a response was required to indicate whether the probe matched an item from the memory set. Participants were encouraged to respond both accurately and quickly. Probe responses were indicated by pressing one of two buttons on a handheld response box, and were followed by a 2.5-s delay, then feedback for 2.0 s indicating the reward received on that trial. On reward trials, correct responses made before the cut-off time were followed by visual feedback indicating the reward received (i.e., "+75 CENTS" or "+25 CENTS", depending on the reward cue). Conversely, incorrect responses or those slower than the cut-off time were followed by visual feedback indicating that no reward was received ("- -"). On non-incentive trials in R+ blocks and trials in R- blocks, correct responses were followed by a neutral message ("Next Trial Coming Up"). Cut-off times were individually set for each participant, based on their own median correct reaction time on trials performed in the nonreward block. The next trial started after the intertrial interval lasting 2.5–7.5 s with 2.5-s steps. Total monetary rewards were paid to the participants after the experiment. Participants were practiced on the task before the experimental sessions.

The present study employed a mixed blocked and event-related fMRI design that enabled independent and simultaneous extraction of transient and sustained brain activity (ref. 4; Fig. 1*A*; see also fMRI procedure). Two types of task blocks were administered, the rewarding block (R+) and nonrewarding block (R-). The rewarding block consisted of three types of pseudorandomly intermixed trials: high reward trials (R+H), low reward trials (R+L), and nonreward trials (R+N), whereas the nonincentive block consisted of only nonreward trials (R-N). Because this study mainly focused on differences in the nonreward trials between R+ and R- blocks, in the main text, the R+N and R-N trials were referred to R+ and R- trials, respectively, but otherwise reward value is explicitly indicated (i.e., R-N, R+N, R+L, or R+H). The first trial of the R+ block never contained a R+N trial, and the R+N trials always followed a reward trial (R+L or R+H). Each task block consisted of 10 trials and lasted 167.5–180 s, interleaved by fixation blocks lasting 50 s. One R+ block involved 2 R+N trials, 4 R+L trials, and 4 R+H trials. Each functional run consisted of two task blocks involving the same condition, and two functional runs were administered for each of the conditions.

Personality Assessment. To assess dispositional traits related to sensitivity to rewards occurring in daily life, three standardized personality assessments were administered to each participant. One assessment was the Behavioral Activation System and Behavioral Inhibition System, which assesses reactivity to reward and penalty cues and their effects on emotional and behavioral responses (BAS/BIS; ref. 5). The second one was the Generalized Reward and Punishment Expectancy Scale, which assesses global expectation of the likelihood of rewards and penalties accruing (GRAPES; ref. 6). The last one was the Regulatory Focus Questionnaire, which assesses the tendency to capitalize on opportunities for reward and avoid penalizing outcome (RFQ; ref. 7). Although each of these three assessments provides one scale for reward traits and another one for penalty traits, only the reward scales were used in the analysis because the present study focused on reward sensitivity. These three assessments measure similar personality traits on one hand, but examined distinct aspects of the reward-related trait on the other hand (i.e., sensitivity for reward cue in BAS, expectation of reward in GRAPES, and promotion goal by reward in RFQ). The present study aimed to examine individual variability in a more general reward-related trait, rather than specific aspects associated with any one scale. Consequently, we computed a composite index, termed "reward sensitivity", based on all three scales, following an approach used previously in personality research (8). The reward sensitivity score for each individual participant was defined as the average of the z scores of the three assessments (z score was calculated for each score and participant). Z score averaging is a standard psychometric procedure that maximizes generality and minimizes statistical distortion in individual variability with small sample sizes (8). Note that the mean and standard deviation of the three personality scores were within normal range (see also Results), indicating that sample biases should be minimal. One participant was excluded from reward-sensitivity analyses because of a score in the outlier range.

fMRI Methods. Scanning was conducted on a head-dedicated Siemens 3-T Allegra System. A pillow and tape was used to minimize head movement in the head coil. Headphones dampened scanner noise and enabled communication with participants. Both struc-

tural and functional images were acquired from each participant. High-resolution structural images were acquired by using an MP-RAGE T1-weighted sequence [repetition time (TR) = 9.7 s; echo time (TE) = 4.0 msec, flip angle (FA) = 10 deg, slice thickness = 1 mm; in-plane resolution = 1×1 mm^2]. Functional images were acquired by using an asymmetric spin-echo echo-planar imaging (TR = 2.5 s; TE = 25 msec; FA = 90 deg; slice thickness = 4 mm; in-plane resolution = 4×4s mm^2; 32 slices) in parallel to the anterior-posterior commissure line, thus allowing complete brain coverage at a high signal-to-noise ratio. Each scanning run consisted of two task blocks alternating with three fixation blocks. During the task block, intertrial interval was variable from 2.5 to 7.5 with 2.5-s steps to obtain temporal jitter required to deconvolve event-related fMRI response. The first four images in each run were excluded from analysis to ensure equilibrium of longitudinal magnetization. Two scanning runs were administered for each of the R+ and R- conditions.

Data Analysis. All functional images were first temporally aligned across the brain volume, corrected for movement by using a rigid-body rotation and translation correction (9, 10), and then registered to the participant's anatomical images to correct for movement between the anatomical and function scans. The data were then intensity normalized (to an arbitrary value of 1,000), resampled into 3-mm isotropic voxels, and spatially smoothed with a 9-mm FWHM (full width, half maximum) Gaussian kernel. Participants' structural images were transformed into standardized Talairach atlas space (11) by using a 12-dimensional affine transformation. The functional images were then registered to the reference brain by using the alignment parameters derived for the structural scans.

Sustained and transient effects were simultaneously but independently coded within the same GLM, enabling dissociation of these effects (4). The logic of the GLM estimation is that event-related effects will decay back to baseline during the ITI, whereas sustained effects should remain relatively constant, and of increased amplitude relative to control (fixation) blocks. This approach has been also validated via both simulation and empirically based methodological studies (4). Given this simultaneous GLM coding for the sustained and transient events, the baseline state in the GLM reflects activity during the 50-s fixation blocks that are interleaved with the task blocks, thus assuring a stable estimate of baseline activation levels. For the sustained effect, the two types of task block (R+ and R-) were coded by a box-car function using an assumption of a fixed-shape response of long duration (i.e., boxcar convolved with a gamma function; ref. 12). For the event-related effects, two types of trials of interest (R+N and R-N trials), together with noninterest trial types (R+L, R+H, and error) and transient effects during block transition (13, 14), were separately coded by using a series of regressors along the hemodynamic response epoch for a trial. The duration of this epoch was 30 seconds (i.e., 12 time points/regressors), given the 12-s duration of one WM trial. Note that these 12 time points for transient effects were statistically independent and individually estimated in the GLM. Further, the delta-function method of estimation for transient events reduces multicollinearly between transient event and sustained events, compared with convolving transient events with hemodynamic response functions (15), because the transient regressors are more sparsely distributed within a task block. More specifically, the correlation between the sustained regressor and each timepoint (frame) estimate of the transient effect averages less than 0.22 and 0.10 in the R- and R+ conditions, respectively. These magnitudes are less than half of those reported in previous studies (15). Thus, any negative correlation between transient and sustained activity (see Fig. 2*D*) should not be attributable to the collinearity. Linear drifts within each functional run and constant signal shifts across the runs were also included as covariates of no interest in the GLM. These regressors were used in place of a high-pass filter, because such filtering may have a tendency to distort the relationship between sustained and transient effects.

The event-related and sustained estimates for the imaging data were then submitted to a group analysis by using a voxel-wise random-effects model. The primary analysis of interest was based on the comparison between R+ and R- trials/blocks. Note that only nonrewarding trials were compared for transient effect. Whole brain exploratory analysis was first performed to identify brain regions that revealed a shift in brain activity dynamics between R+ and R- block/trials in terms of sustained and transient effects. Specifically, this shift in dynamics was tested by the conjunction of the following two contrasts: (*i*) a significant difference in sustained activity during R+ and R- block ($P < 0.01$) and (*ii*) a significant trial by time effect for the transient activity during the R+ and R- trial ($P < 0.01$). Then voxel clusters identified by the conjunction were assessed for significance by using the AlphaSim Monte Carlo procedure (http://afni.nimh.gov/afni/). This procedure estimates the statistical significance of voxel clusters at various sizes by simulating cluster occurrences under random distributions within a region mask. A rigorous threshold was used, $P < 0.05$ corrected for multiple comparisons across the whole brain. Importantly, brain regions were reported significant only if the conjunction null hypothesis was rejected (i.e., rejection rate was controlled by the larger *P* value in the two contrasts; ref. 16).

Region-of-interest (ROI) analyses were then performed to examine profiles of the activity dynamics for each ROIs. Because each trial of the present WM paradigm consisted of multiple events (i.e., reward cue, encoding, delay, probe, feedback), two activity components of interests were extracted from the time course of the transient effect (see ref. 17 for similar approach). One is the early-trial component, defined as the differences in parameter estimates between the average of frame 2 and 3 and the average of the 1, 10, 11, and 12, and the other is the late-trial component, defined as the differences in parameter estimates between the average of frame 4, 5, and 6 and the average of the 1, 10, 11, and 12.

The within-trial decomposition of the activity timecourse is statistically appropriate because, as stated above, the signal magnitude of each time point was estimated based on statistically independent regressors (4). With the time constant of the hemodynamic response (3–6 s), the early-trial component likely includes activity that is primarily related to the presentation of reward cue and encoding of the word set, whereas the late-trial component primarily includes maintenance of the word set and the response to the probe but likely not any reward feedback effects. Although some of the activation level in the late component may have been influenced by the bleeding-over effect of BOLD signal from the early component, statistical dissociation is still possible (18). Further, the early-late division corresponds well to the distinction of proactive-reactive control, because proactive control should affect both transient updating processes occurring during memory set presentation, and anticipatory maintenance of attentional expectancies regarding the probe. In contrast, reactive control should affect the reaccess of goal-related information at the time of the probe to enable successful response selection.

Trial-related effects of reward value were also examined. For R+N, R+L, and R+H trials, transient activity was decomposed into early and transient periods, with an identical procedure as stated above. Then a one-way repeated-measure ANOVA was performed to test whether each transient component was modulated according to the trial reward value. Note that, because nonreward trials in the R+ block (R+N) were intermixed with reward trials (R+L, R+H), reward-related effects may have been maintained and/or carried over into nonreward trials. Nevertheless, these carry-over effects are still appropriately referred to as "context effects".

Brain–Behavior Relationship Analysis. Voxel-wise Pearson correlation coefficients were computed between the behavioral or per-

sonality measurements and activity components. In analyses involving RT data, the R+ context effect was estimated by partialling out the RT in R- trials from the R+ trials (i.e., the residual of a simple regression was used). A separate analysis used RT data related to trial reward value. In this analysis, the correlation was calculated between RT enhancement and brain activity in the ROI during R+H, R+L, and R+N trials by using similar procedures. Voxel clusters identified in correlational analyses were then assessed for significance by using the Monte Carlo procedure within the ROI identified in the whole brain analysis. Significant correlations were reported above the threshold of $P < 0.05$, corrected for multiple comparisons by using the Monte Carlo procedure within the ROI.

In the mediation analysis, the independent (predictor) and dependent (predicted) variables were the reward sensitivity score and the reaction time (RT) enhancement in the R+N trial, respectively. The present model constitutes a single mediator model, with the mediator consisting of two activity components (Fig. 4*A*). Specifically, one component consists of the sustained activity and early transient activity, and the other component consists of late transient activity. These components constitute a single but step-wise mediator based on the temporal order of the task. In a separate control analysis, another model was tested by reversing the casual relationship of the activity components (i.e., the late-task effect was predicted by the reward sensitivity score, and the sustained/early-task effect predicts the behavioral performance; Fig. S5*B*). Additionally, models with only one component mediator were tested to examine whether each of the activity components sufficiently explained behavioral variability in both of the RT and reward-sensitivity score (Fig. S6).

Each activity component was extracted from the set of voxels that exhibited a conjunction effect of the three correlations within the ROI identified in the whole brain exploratory analysis: (*i*) sustained activity and reward sensitivity score, (*ii*) early transient activity and reward sensitivity score, and (*iii*) late transient activity and RT. These activity components were contrasted between R+ and R- trials/blocks before statistical testing. Then, the early transient activity and sustained activity was averaged within participants, and the late-transient activity was orthogonalized to the early-related activity by using regression residuals to eliminate a bleeding-over effect from the early component due to serial autocorrelation in the BOLD signal. For the RT, the regression residual of the RT in the R+ trial was used by partialing out the RT in the R- trial. A critical statistical test in the mediation analysis is the significance of the indirect effect from the reward sensitivity to RT via the brain activity components. All of the regression coefficients in the model were estimated simultaneously in a multivariable regression. The indirect effect was tested by using the bootstrap procedure (19), with the bias-corrected confidence-interval procedure implemented in Amos 17.0 (SPSS) repeated in 2000 samples (20). Regression coefficients were tested by using a maximum likelihood method and also confirmed by using the bootstrap procedure for consistency.

To examine whether the indirect effect was unusually inflated by the definition of the lPFC region of interest (i.e., conjunction of the three correlation contrasts), a supplementary analysis was performed in which the lPFC ROI was identified independently of the correlation. Specifically, brain regions were extracted by using a conjunction of two contrasts: (*i*) significant difference in sustained activity during R+ block and R- block ($P < 0.001$) and (*ii*) significant trial by time effect for the transient activity during the R+ and R- trials ($P < 0.001$). Then voxel clusters identified by the conjunction were assessed for significance by using Monte Carlo procedure ($P < 0.05$, corrected for multiple comparison for the whole brain with conjunction null hypothesis; ref. 16). Identical procedures were employed to estimate and test regression coefficients and indirect effect. Alternative, control models (see above) were also tested by using this dataset. To quantitatively compare the alternative models, χ^2 tests were performed. Further, Adjusted Goodness of Fit Indices (AGFI; determination coefficient adjusted by the degree of freedom in the model; ref. 21) were inspected.

To demonstrate personality-dependent activity dynamics during R+ trials, each activity component was calculated based on the reward-sensitivity score. The magnitudes for sustained, early-transient, and late-transient activity was averaged within 10 highest and lowest score participants and then separately plotted along the temporal axis. The signal magnitude represents the activity increases relative to the fixation block and, thus, the baseline of the transient effects is their sustained effects.

SI Results

Behavioral Results. ***Accuracy.*** Accuracy of the task was high, >95% correct for all conditions: 96.5 ± 4.0% (mean ± SD) for R+N trial, 96.0 ± 6.1% for R-N trial, 95.5 ± 7.0% for R+L trial, and 98.3 ± 3.2% for R+H trial. A one-way repeated measures ANOVA was performed with the types of trial (R-N, R+N, R+L, R+H) as the factor. The main effect was not significant [$F_{(3,90)} = 2.10, P = 0.11$], probably due to a ceiling effect. Percent reward rate for the R+H and R+L trials were 87.3 ± 13.1%, indicating that the participants were well-rewarded during the R+ block by improving their behavioral performance. The reaction times (RTs) were 945.5 ± 211.3 ms for R-N trial, 752.0 ± 180.4 ms for R+N trial, 722.98 ± 149.9 for R+L trial, and 685 ± 154 ms for R+H trial (Fig. S2*A*).

Personality assessments. The personality score of the reward-sensitivity trait was 40.9 ± 5.3 for the Behavioral Activation System and Behavioral Inhibition System (BAS/BIS), 8.9 ± 2.3 for Generalized Reward and Punishment Expectancy Scale (GRAPES), and 23.7 ± 3.3 for Regulatory Focus Questionnaire (RFQ), respectively. All of the mean scores were within normal ranges (5–7). The reward sensitivity score was then calculated by averaging the z scores of each personality score within individual participants (*Methods*). One participant was excluded in individual differences analysis because of an outlier score (2.8). The resulting mean score was 0.08 ± 0.72. The score ranged from −1.20 to +1.40.

Correlation between personality and performance. In addition to the primary correlations between reward-sensitivity and the behavioral reward context effect reported in the primary text, additional correlational analyses were also conducted with the behavioral trial reward value effect. Partial correlations examined the relationship between reward-sensitivity and RT facilitation in the R+L and R+H trials (controlling for R+N and/or R+L performance). None of the correlations were significant ($|r| < 0.23, P > 0.23$) (Fig. S2 *B* and *C*). These results suggest that the reward sensitivity trait is reflected in contextually-based behavioral enhancement during the R+ block, rather than trial-by-trial effects of reward value.

Imaging Results. We examined the effects of contextual and trial reward value on both sustained and transient activation in the right lateral prefrontal cortex lPFC region identified in the whole brain exploratory analysis (Fig. S3*A*). For transient effects, activation in R+N, R+L, and R+H trials was significant during the early-trial period, (R+H: $t_{(30)} = 2.9$, $P < 0.01$; R+L: $t_{(30)} = 4.1$, $P < 0.001$; R+N: $t_{(30)} = 3.0$, $P < 0.001$), but not during the late-trial period [$t < 1.6; P > 0.10$]. In both periods, the magnitude did not show an effect of trial type (EARLY: $F_{(2,60)} = 1.4$, $P = 0.26$; LATE: $F_{(2,60)} = F_{(2,60)} = 0.28$, $P = 0.76$). Importantly however, the difference between early and late transient period was also significant ($F_{(1,30)} = 4.4, P < 0.05$), suggesting significant deflection in the late period independent of reward value. A direct examination of the timecourse data shows similar magnitude and temporal pattern, with larger transient activity during early-transient period, but larger deflection during late-transient period (Fig. S3*B*).

Brain and behavior relationships. To further examine whether PFC activity dynamics were modulated by trial reward value effects on RT, voxel-wise correlations were conducted between late-trial transient activation and the trial reward value RT facilitation effect (R+H vs. R+L and R+L vs. R+N) within the lateral PFC

region of interest. As shown in Fig. S4, no significant clusters of correlated voxels were identified.

Parietal region. To examine whether the parietal region identified in the whole brain exploratory analysis (Table S1) exhibited similar effects as observed in the lPFC ROI, correlations were examined between the parietal activity (sustained, early transient, and late transient) and behavioral measurement (RT facilitation or reward sensitivity score). No significant correlation was observed.

Mediation analysis. In addition to the primary mediation analyses reported in the main text, supplementary analyses were also conducted to examine the robustness of the present mediation effect (*Methods*). In one analysis the region of interest was identified independently of any brain–behavior correlations (see *Methods* for definition). A single focal lPFC region was identified [Tarairach coordinate: (42, 30, 22); 20 voxels]. As shown in Fig. S5*A*, the model successfully explained the data ($\chi^2 = 1.7, P = 0.42$; AGFI = 0.85), and more critically, the significant indirect effect and regression coefficients were again confirmed (indirect effect: $\beta = -0.06$, $P < 0.05$; regression coefficients: all βs, $P < 0.05$). Additional analyses tested control (null) models, which examined the specificity of the causal paths. As shown in Fig. S5*B*, if the causal direction of the sustained/early-transient and late-transient effects are reversed, the model fails to fit the data ($\chi^2 = 9.8$, $P < 0.01$; AGFI = 0.30). Accordingly, the indirect effect also failed to reach significance ($P = 0.77$), whereas the direct effect remained significant ($P < 0.05$). Finally, as shown in Fig. S6, both path components need to be included for the mediation effect to be reliable. If the sustained/early-transient or late-transient effect is eliminated from the model, the mediation indirect effects are no longer significant ($P > 0.17$).

1. Balota DA, et al. (2007) The English Lexicon Project. *Behav Res Methods* 39:445–459.
2. Lund K, Burgess C (1996) Producing high-dimensional semantic spaces from lexical co-occurrence. *Behav Res Methods* 28:203–208.
3. Cohen JD, MacWhinney B, Flatt M, Provost J (1993) PsyScope: An interactive graphic system for designing and controlling experiments in the psychology laboratory using Macintosh computers. *Behav Res Methods Instrum Comput* 25:257–271.
4. Visscher KM, et al. (2003) Mixed blocked/event-related designs separate transient and sustained activity in fMRI. *Neuroimage* 19:1694–1708.
5. Carver CS, White T (1994) Behavioral inhibition, behavioral activation, and affective responses to impending reward and punishment: The BIS/BAS scales. *J Pers Soc Psychol* 67:319–333.
6. Ball SA, Zuckerman M (1990) Sensation seeking, Eysenck's personality dimensions and reinforcement sensitivity in concept formation. *Pers Individ Dif* 11:343–353.
7. Higgins ET, et al. (2001) Achievement orientations from subjective histories of success: Promotion pride versus prevention pride. *Eur J Soc Psychol* 31:3–23.
8. Zelenski JM, Larsen RJ (1999) Susceptibility to affect: a comparison of three personality taxonomies. *J Pers* 67:761–791.
9. Friston KJ, Williams S, Hward R, Frackowiak RSJ, Turner R (1996) Movement-rlated effects in fMRI time-series. *Magn Reson Med* 35:346–355.
10. Snyder AZ (1996) in *Quantification of Brain Function using PET*, eds Baller D, Jones T (Academic, San Diego).
11. Tarairach J, Tournoux P (1988) *Co-planar Stereotaxicc Atlas of the Human Brain* (Thieme Medical Publishers, New York).
12. Boynton GM, Engel SA, Glover GH, Heeger DJ (1996) Linear systems analysis of functional magnetic resonance imaging in human V1. *J Neurosci* 16:4207–4221.
13. Konishi S, Donaldson DI, Buckner RL (2001) Transient activation during block transition. *Neuroimage* 13:364–374.
14. Dosenbach NUF, et al. (2006) A core system for the implementation of task sets. *Neuron* 50:799–812.
15. Otten LJ, Henson RN, Rugg MD (2002) State-related and item-related neural correlates of successful memory encoding. *Nat Neurosci* 5:1339–1344.
16. Nichols T, Brett M, Anderson J, Wager T, Poline J-B (2005) Valid conjunction inference with the minimum statistic. *Neuroimage* 25:653–660.
17. Fox MD, Snyder AZ, Vincent JL, Raichle ME (2007) Intrinsic fluctuations within cortical systems account for intertrial variability in human behavior. *Neuron* 56:171–184.
18. Yarkoni T, Speer NK, Zacks JM (2008) Neural substrates of narrative comprehension and memory. *Neuroimage* 41:1408–1425.
19. Shrout PE, Bolger N (2002) Mediation in experimental and nonexperimental studies: new procedures and recommendations. *Psychol Methods* 7:422–445.
20. Shamosh NA, et al. (2008) Individual differences in delay discounting: relation to intelligence, working memory, and anterior prefrontal cortex. *Psychol Sci* 19:904–911.
21. Mulaik SA, et al. (1989) Evaluation of good-of-fit indices for structural equation models. *Psychol Bull* 105:430–445.

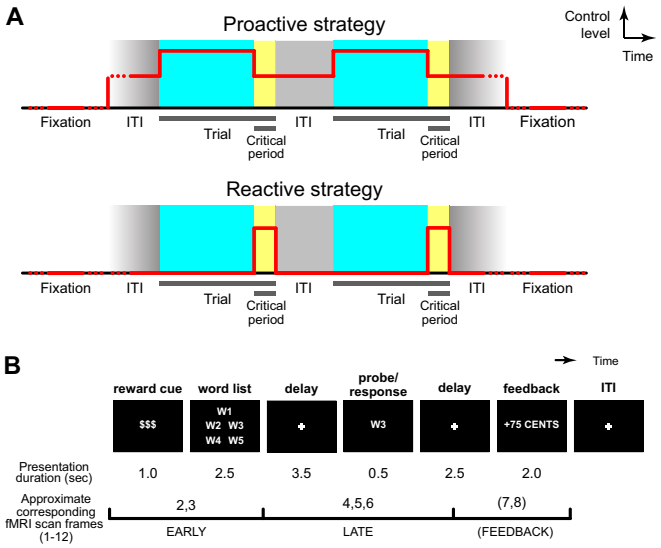

Fig. S1. (*A*) Schematic illustration of theoretical framework distinguishing proactive control (*Upper*) and reactive control (*Lower*) in terms of putative temporal dynamics. Horizontal and vertical axes indicate time and control engagement level, respectively. Proactive control is characterized by (*i*) sustained control during the intertrial-interval (ITI), and (*ii*) transient preparatory control at the early period of the task trial. In contrast, reactive control is characterized by transiently increased control at the critical period of each trial (e.g., around response periods) but low levels of sustained and preparatory transient control. Strategy shifts from reactive to proactive control should be characterized by a neural signature in which sustained and transient preparatory control is increased, but late-trial reactive activity is relatively decreased. (*B*) Participants performed a working memory task in which a reward cue was presented at the beginning of each trial, which indicated the potential reward available for fast and correct responses. Durations of presentation for each set of stimuli were indicated below. Approximate fMRI scan frames in the transient effect were indicated at the bottom with the labels (EARLY, LATE) referred in the text.

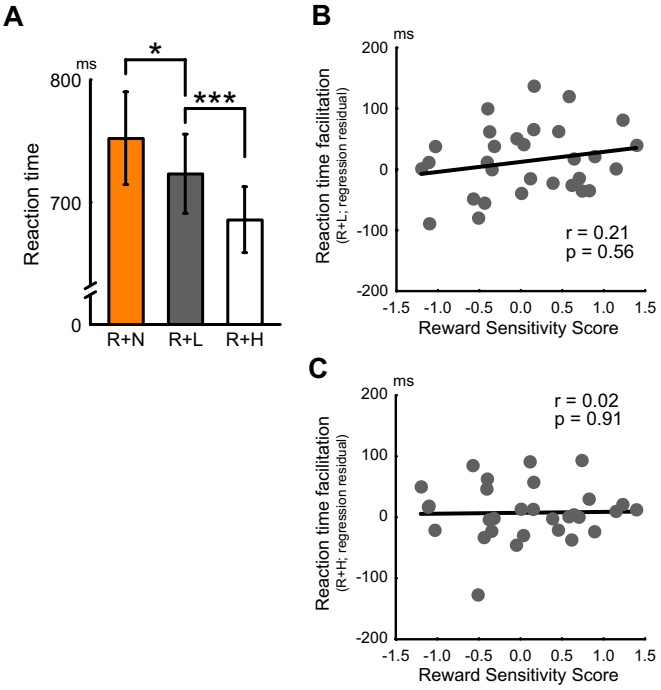

Fig. S2. Reaction times for different trial types in the R+ block. (*A*) Reaction times were faster on reward trials and also modulated by the magnitude of the reward. R+N, nonreward trial; R+L, low-reward trial; R+H, high-reward trial. Reward sensitivity score does not correlate with reaction time facilitation during R+L trials (*B*) or R+H trials (*C*). **, $P < 0.01$; *, $P < 0.05$.

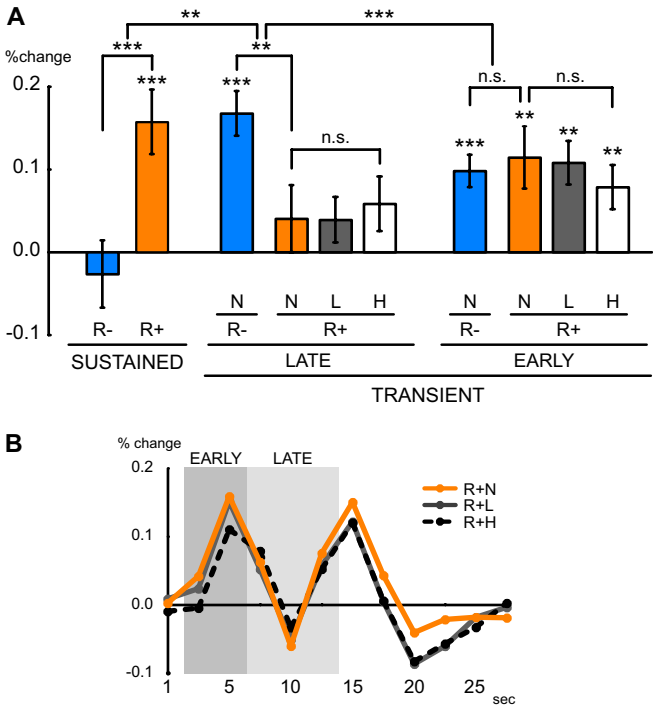

Fig. S3. Sustained and transient activity in the right PFC region. (*A*) Sustained estimates are shown for the nonrewarding (R-; blue), and rewarding (R+; orange) blocks. Transient estimates during each of the early and late task periods are also shown for the nonreward trials in the R- block (N; blue), and for nonreward (N; orange) low-reward (L; gray) and high-reward (H; white) trials for the R+ block. ***, $P < 0.001$; **, $P < 0.01$; *, $P < 0.05$. n.s., not significant. (*B*) Transient effects during the R+ block. Time courses shown for nonreward trials (R+N; orange), low-reward trials (R+L; gray), and high-reward trials (R+H; black dashed).

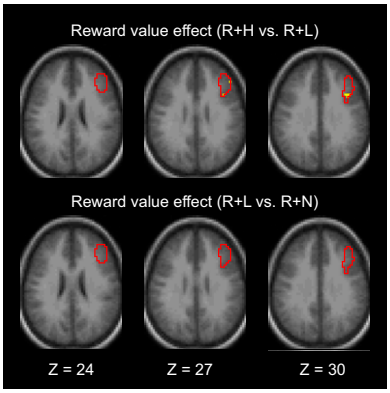

Fig. S4. Statistical correlation maps between reaction time (RT) facilitation related to trial reward value and late-transient activity. Voxels showing correlation ($P < 0.05$ uncorrected; a liberal threshold was used to show the null results) were colored in yellow on the transverse anatomical section at labeled coordinate. The area enclosed by red lines indicates PFC ROI identified in whole brain exploratory analysis. There were no significant clusters voxels within the PFC ROI showing correlations between activity and RT facilitation on either R+H trials (*Upper*) or R+L trials (*Lower*).

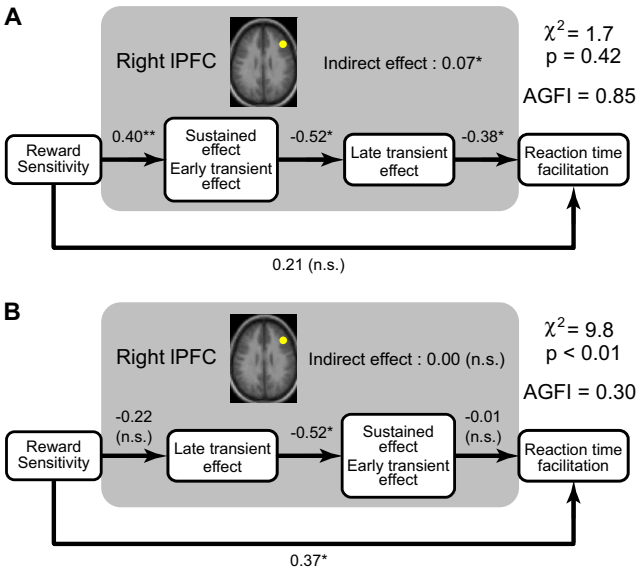

Fig. S5. Control mediation analyses. (*A*) A significant indirect effect was still observed when the PFC mediation region was defined independently of correlations between brain activity and behavioral measurements (*Methods*). (*B*) In another model, with the causal relation between the sustained/early-transient and late-transient effects reversed, the model failed to fit the data. The indirect effect was not significant, whereas the direct effect remained significant. **, $P < 0.01$; *, $P < 0.05$. AGFI, adjusted goodness of fit index.

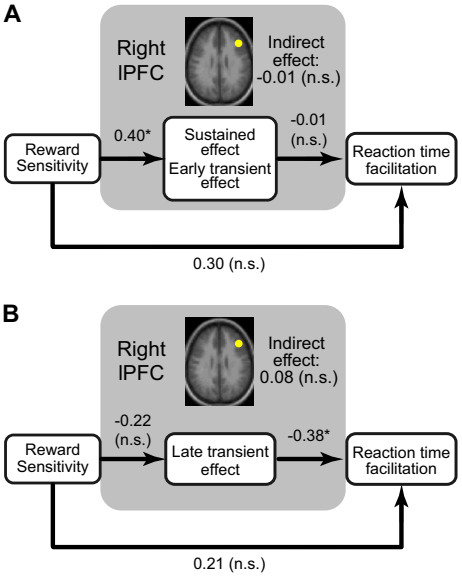

Fig. S6. Additional control mediation models with only a single activity component. (A) Mediation model with only sustained/early-transient component. (*B*) Mediation model with only late-transient effect component. In both models, the indirect effect was not significant. *, $P < 0.05$.

Table S1. Brain regions showing significant shift in activity dynamics between the R+ and R- trial/block

		Coordinate						
Area	L/R	*x*	*y*	*z*	BA	Cluster size	Sustained effect $t_{(30)}$	Transient effect $F_{(11,\ 330)}$
Lateral Frontal	R	41	21	28	46/9	212	3.90*	3.84*
Posterior Parietal	R	39	−51	47	7/40	197	4.15*	6.41*

Coordinates are the center of the cluster and listed in the Tarairach space (12). BA is the Brodmann area near the coordinates and is approximate. The size of cluster was indicated by the number of voxel. *, $P < 0.001$.